Adaptive CSOGI-Based synchronization using neural networks for distorted Grid conditions

Ilias EN-NAOUI[1*], *Azeddine* MOUHSEN[1], *Abdelhadi* RADOUANE[1] and *Aymen BOUJEMEL*[1]

[1]Laboratory of Energy-Matter-Instrumentation & Telecoms (EMIT), Faculty of Sciences and Techniques, Hassan First University, Settat, Morocco

Abstract. Phase-Locked Loops (PLLs) are widely used in grid-connected systems for accurate phase and frequency estimation. Their performance greatly depends upon the quality of the preconditioning stage, particularly in non-ideal grid conditions. For improved robustness, a double cascaded second-order generalized integrator (CSOGI) is often utilized to obtain in-phase and quadrature clean signals from the input one. Though effective, the conventional CSOGI is founded on fixed design parameters, thereafter with limited capability in handling of time-varying disturbances. An adaptive synchronization method is introduced in this work, through which the CSOGI filtering gain is adaptively controlled in real time by an artificial neural network (ANN). The design CSOGI-ANN structure supports better dynamic response and improved harmonic rejection.

1 Introduction

Power electronic converters are central to the integration of renewable energy sources in modern electrical grids [1, 2] as demonstrated in Fig.1. The converters depend heavily on reliable and accurate synchronization mechanisms to synch their operation with voltage characteristics of the grid, including phase, frequency, and amplitude [3].

Phase-locked loops (PLLs) are the main target of synchronization methods for three-phase systems. The Synchronous Reference Frame PLL [4, 5] (SRF-PLL) is used most frequently because it is simple to implement on digital platforms and ensures stable operation under perfect, balanced grid conditions. Its performance is critically impacted when the grid voltage is exposed to realistic disturbances. The SRF-PLL, for example, is sensitive to DC offsets, voltage unbalance and harmonic distortion [6-8].

A more robust alternative is the double cascaded second-order generalized integrator [9], [10] (D-CSOGI) topology. As two cascaded SOGI filters, it is a developed signal conditioning stage that generates clean quadrature and in-phase signals from distorted input voltages. Although being more reliable, the conventional CSOGI is designed with fixed filter parameters [7],[11],[12]. Real-world operating conditions are far from static conditions in a grid. Voltage amplitude, frequency, and harmonic content can all change over time. A design with fixed parameters cannot provide best filtering in these cases.

* Ilias EN-NAOUI: i.ennaoui@uhp.ac.ma

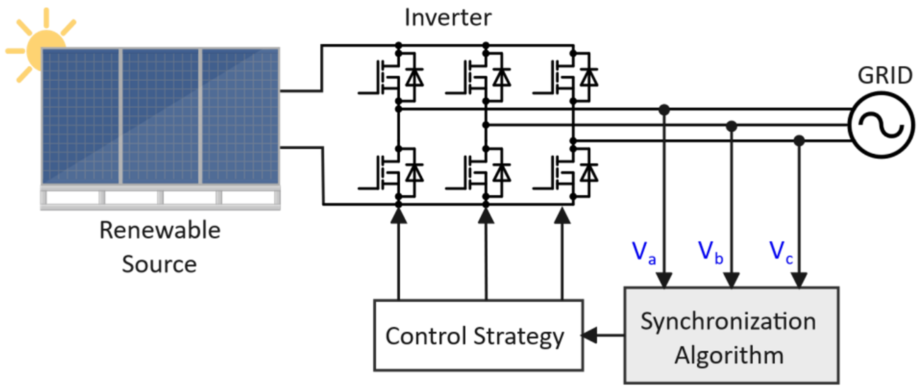

Fig. 1. System Architecture.

To overcome this drawback, this study proposes an adaptive CSOGI structure where filtering action adaptively varies in real time in accordance with the grid condition at the moment. This structure transforms the system from a fixed setting into an intelligent and self-tuning synchronization mechanism with the capability to maintain high performance under a wide range of grid perturbations.

In this work, we propose an advanced, three-phase synchronization system wherein the conventional CSOGI structure is artificially adjusted by artificial neural networks (ANN). The system takes advantage of the learning feature of neural networks whereby the CSOGI block's parameters are adjusted in real time based on the grid's state at any instance. This adaptive function eliminates low and high-order harmonics as well as DC offset terms from the input signal.

This paper is organized as: The first part overviews the conventional CSOGI structure and describes its performance limitations under time-varying grid conditions. It also introduces the proposed CSOGI-ANN system, which adjusts its filtering characteristics, such as bandwidth and dynamic response, according to real-time grid changes. The second section provides a set of simulation-based test cases used to contrast the performance of the conventional CSOGI structure and the proposed adaptive method for various grid conditions. In the final section, the paper is concluded by highlighting the major findings and proposing potential directions for future improvement and validation.

2 Methods

D-CSOGI architecture, introduced in previous works [12], is an advanced block for positive sequence extraction. The architecture relies on two CSOGI blocks for the rejection of harmonics and DC offset while also delivering the in-phase and quadrature elements of the grid voltage. Its output is subsequently passed to an SRF-PLL in order to achieve precise estimation of phase and frequency. In this work, the conventional CSOGI is enhanced by incorporating ANNs to dynamically adjust its parameters in real time in order to improve the filtering performance under variable grid conditions.

2.1 The Conventional CSOGI structure

The proposed system is based on a D-CSOGI operating in the stationary αβ frame. After ADC conversion, the three-phase voltages V_{abc} are transformed into orthogonal components V_α and V_β, each one is processed through a CSOGI block to extract the fundamental positive sequence. As shown in Fig. 2, the conventional CSOGI generates two outputs V_S and qV_S.

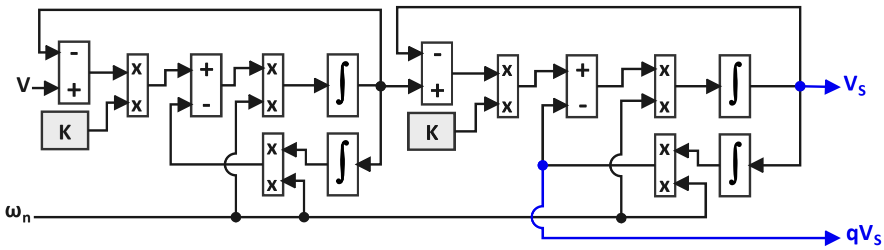

Fig. 2. Internal structure of the CSOGI filter.

These signals represent the filtered components of the input grid voltage, in phase and in quadrature, respectively, relative to the fundamental frequency. The relationship between the CSOGI's input signal V and the outputs is defined by two transfer functions, D(s) and Q(s) described by equations (1) et (2).

$$D(s)=\frac{V_s(s)}{V(s)}=\frac{(k.\omega_n.s)^2}{(s^2+k.\omega_n.s+\omega_n{}^2)^2} \tag{1}$$

$$Q(s)=\frac{qV_s(s)}{V(s)}=\frac{k^2.\omega_n{}^3.s}{(s^2+k.\omega_n.s+\omega_n{}^2)^2} \tag{2}$$

As can be seen from the provided figure and as shown by the transfer functions, the sole design parameter that can be employed in this structure is the gain *k*, and it has a direct impact on the bandwidth of the system, and thus its dynamic response. As shown in figure Fig.3, the filtering bandwidth and response time of the structure are observed to change as a function of different values of gain *k.* It can be observed that a greater gain gives a faster dynamic response but reduces the filtering capacity of the structure. A reduction in *k* improves harmonic rejection at the cost of response time.

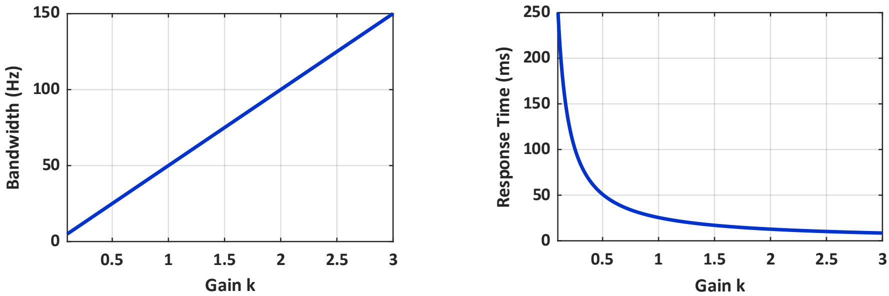

(a) (b)

Fig. 3. The impact of the gain k on (a) bandwidth and (b) response time of the CSOGI structure.

But the techniques described in the above-cited literature [13] are founded on a static design of gain *k*, and thus the parameter is invariant irrespective of the grid's conditions. The static setting has the limitation for the adaptability of the CSOGI under grid changes from highly distorted to well-balanced and clean conditions. Thus, the structure can have either a response that is too slow or have weak filtering capabilities, depending on the specific scenario.

2.2 The proposed CSOGI-ANN system

In order to surmount the constraints imposed by static gain selection, we propose an adaptive tuning strategy for the parameter *k* that uses an ANN, as illustrated in Fig.4. The ANN is trained to recognize different grid conditions and dynamically adjust the value of K_{NN} in real time. In scenarios where the grid is distorted, particularly in cases of high and low harmonic content, the ANN reduces the gain K_{NN} with the objective of enhancing the filtering capability of the CSOGI. Conversely, under stable grid conditions, the ANN increases K_{NN} to enhance the system's dynamic response. In this work, a multilayer perceptron (MLP) neural network has been adopted to dynamically adjust the gain K_{NN} of the CSOGI structure based on real-time grid conditions. In order to determine the most efficient architecture, multiple training scenarios were evaluated by varying key parameters [14]. These parameters included the number of hidden layers, the number of neurons per layer, the choice of activation functions and the number of training iterations.

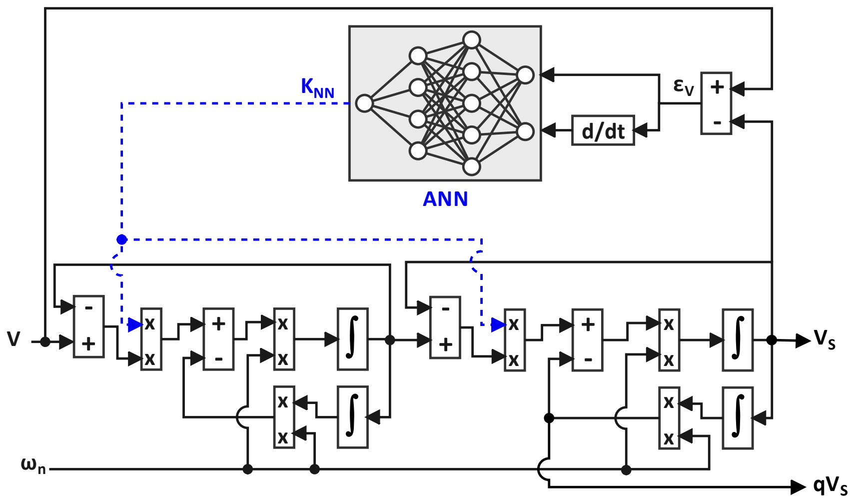

Fig. 4. Block diagram of the proposed CSOGI-ANN structure.

To build the training dataset, a series of simulation scenarios were designed to reflect a wide range of grid conditions, including balanced and distorted states. For each scenario, the input features were computed as follows:

- the instantaneous filtering error, denoted as $\varepsilon_v(t)$, defined in equation (3) as the difference between the input grid voltage $v(t)$ and the in-phase output of the CSOGI $v_S(t)$.

$$\varepsilon_v(t) = v(t) - v_S(t) \tag{3}$$

- and its time derivative ($d\varepsilon_v(t)/dt$), which reflects the dynamic variation of $\varepsilon_v(t)$.

The training dataset was built from a wide range of grid conditions, varying from ideal signals (THD = 0%) to highly distorted ones (THD up to 40%). For each case, the target gain K_{NN} was carefully selected to ensure fast dynamic response and effective filtering by the CSOGI. The selection of K_{NN} was guided by the design insights obtained from figures Fig. 3(a) and Fig. 3(b). The resulting offline dataset captures both steady-state and transient behaviors, enabling the ANN to generalize across diverse grid scenarios.

The ANN implemented in this work is a feedforward structure, which has been designed to model the nonlinear relationship between the input signals and the adaptive gain K_{NN} parameter. Among the different learning algorithms, the Levenberg–Marquardt (LM) algorithm was employed, as it is highly efficient, converges very fast, and it is best for function approximation problems, making it highly appropriate to the nature of regression problems being dealt with in this application. To obtain the best structure of ANN, a set of experiments was conducted. These experiments involved changing the activation functions utilized in every layer (Hidden Layer 1 (HL_1); Hidden Layer 2 (HL_2) and Output Layer (OL)), with the selection of frequently alternatives (Logistic-Sigmoid 'logsig', Hyperbolic-Tangent-Sigmoid 'tansig, and Linear-Transfer Function 'purelin'). Furthermore, both the number of layers and the number of neurons per layer were systematically changed to evaluate the impact on network performance. Mean squared error (MSE) and coefficient of determination (R^2) were computed and compared for every configuration in order to examine the compromise between learning accuracy and generalization capability [15], [16].

The final architecture, trained using the Levenberg–Marquardt (LM) algorithm, is organized as follows, and depicted in figure Fig.5:

- The input layer includes two neurons, which correspond to the filtering error signal ε_v and $d\varepsilon_v(t)/dt$.
- The HL_1 is composed of 2 neurons and uses the logsig activation function.
- The HL_2 contains 4 neurons with the purelin activation function.
- The OL which corresponds to the estimated parameter K_{NN}, consists of one neuron, also using the purelin activation function.

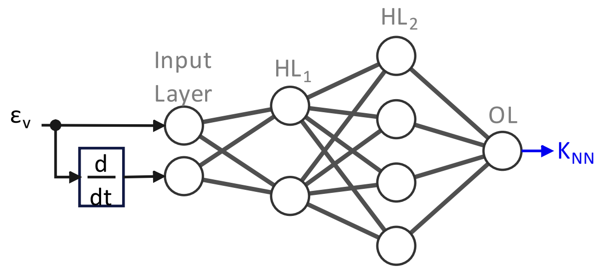

Fig. 5. The chosen structure of the neural network model used in CSOGI-ANN system.

This configuration was selected for the final implementation as it achieved the lowest MSE (3.343×10^{-7}), and a high R^2 value close to 1, and required the fewest training iterations (3252) as depicted in figure Fig.6, demonstrating accuracy and computational efficiency, which make this configuration well-suited for real-time applications where fast convergence and high precision are essential.

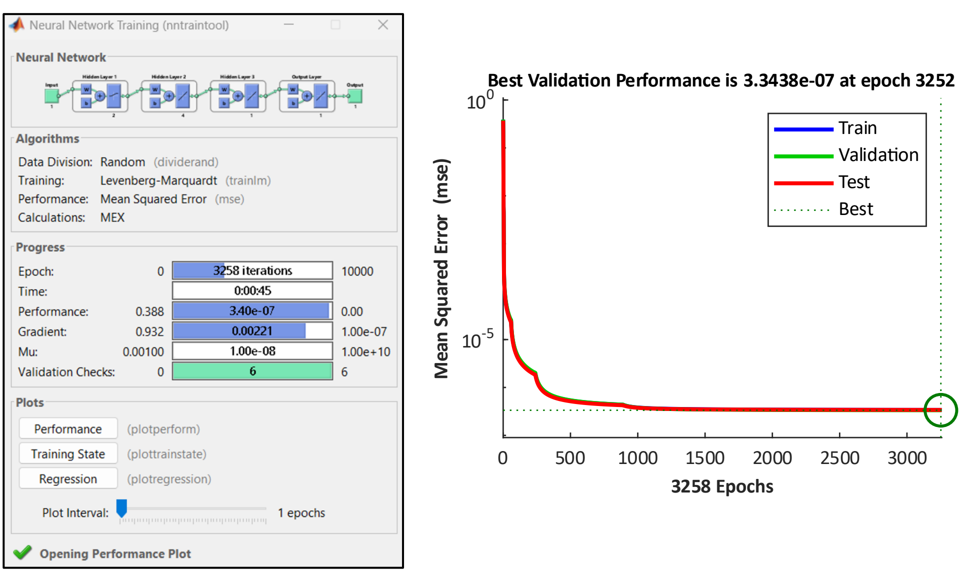

(a) (b)

Fig. 6. Performance of the ANN (a) NN Training tool configuration. (b) MSE convergence curve.

 https://doi.org/10.1051/e3sconf/202568000029

3 Discussions of the obtained results

To evaluate and compare the performance of the conventional CSOGI structure characterized by a fixed, statically designed gain parameter k, as described in [11], [13] (k=1.6), and the proposed adaptive CSOGI-ANN architecture, two test scenarios are conducted. The initial scenario is designed to evaluate the dynamic behavior of both systems under ideal grid conditions. The second scenario introduces significant harmonic distortion in the grid voltage to analyze how each structure responds to non-ideal conditions.

3.1 Test N°1: Balanced grid with a DC offset

This evaluation test compares the performance of both the conventional and proposed CSOGI-ANN structures under balanced grid conditions without harmonic distortion. It is important to note that the voltage waveform shown in Fig. 7(a) represents a conditioned signal used to emulate a digital implementation, rather than the original grid voltage.

A DC offset of 1.5 V is added to emulate the signal conditioning stage, which shifts the grid voltages into the range (0–3.3 V) required for safe analog-to-digital conversion before being applied to a digital processing board such as a DSP. The fundamental grid component has an amplitude of 1V at 50 Hz, corresponding to the scaled version of the original grid voltage. The input voltage waveform utilized in this test is illustrated in figure Fig.7(a).

(a)

(b)

(c)

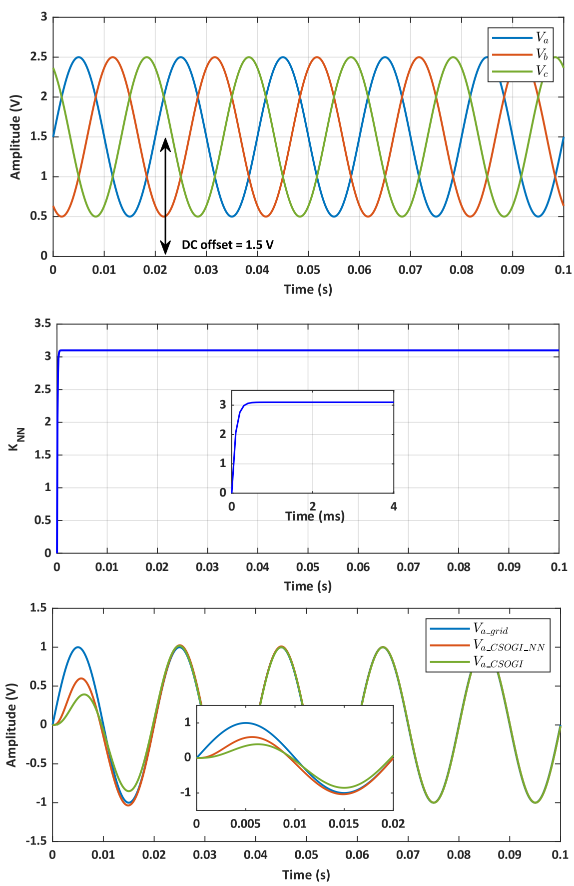

Fig. 7. Balanced grid test: (a) Grid Signals (b) K_{NN} gain (c) CSOGI-ANN versus CSOGI responses.

In this test, the grid voltage is ideal and free of harmonic distortion (THD = 0%). Under these conditions, the neural network rapidly converges to an appropriate K_{NN} gain value of approximately 3.1 within about one millisecond, as shown in figure Fig.7(b). This high gain value ensures a fast dynamic response of the CSOGI block. Figure Fig.7(b) shows how this adaptive gain affects the output signal $V_{a\_CSOGI\_NN}$ of the CSOGI-NN block, converges more quickly than V_{a_CSOGI}, the output of the CSOGI block with fixed gain (k=1.6). Additionally, the system is unaffected by the DC offset in the input because the output signals are purely AC. These results confirm the efficiency of the neural network approach for real-time adaptation of the gain based on grid conditions.

3.2 Test N°2: Balanced grid with a DC offset

In this experiment, the input signal was modified at t=0.1s, by the injection of a 5th harmonic component of 0.2p.u with respect to the fundamental, and a 7th harmonic of 0.15p.u. These additions resulted in a THD of 25%, which characterizes a severely polluted grid condition as depicted in figure Fig.8(a). This scenario was designed to assess and compare the filtering performance of the conventional CSOGI structure, which relies on a statically designed gain parameter, against the proposed adaptive CSOGI-ANN structure.

(a)

(b)

(c)

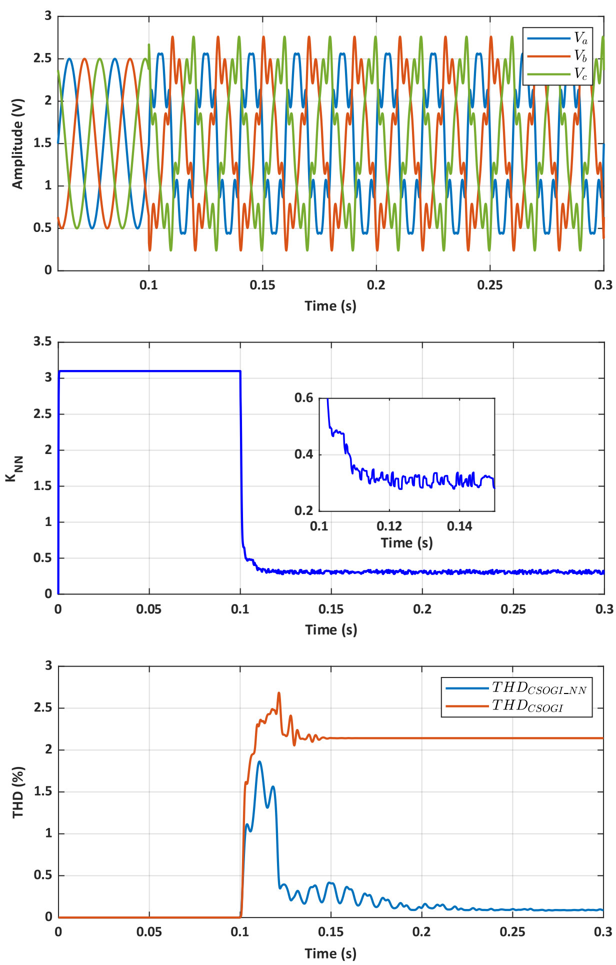

Fig. 8. Distorted grid test: (a) Grid Signals (b) K_{NN} gain (c) THD output of both CSOGI structures.

At the beginning of the test, when the grid voltage is clean and free from harmonic distortion, the neural network assigns a high K_{NN} value of approximately 3.1 as illustrated in figure Fig.8(b). This value enhances the transient response of the CSOGI block under ideal conditions. As the test progresses, the neural network detects the presence of significant harmonic distortion in the grid voltage. In response, it adaptively reduces the gain value to approximately 0.3 around t=0.1s. This adjustment demonstrates the network's ability to adapt its internal parameters dynamically, ensuring better filtering performance and improved harmonic rejection under non-ideal grid conditions. In addition, before the introduction of harmonics at time equal to 0.1 seconds, both systems exhibit negligible distortion as depicted in figure Fig.8(c). However, once the harmonic distortion is injected into the grid, the structure based on a fixed gain design (k=1.6), shows a significant increase in the total harmonic distortion of the output signal, reaching approximately 2.2%. In contrast, thanks to the adaptive adjustment of the gain generated by the neural network, the proposed adaptive structure CSOGI-ANN effectively suppresses the harmonics, resulting in a notably lower total harmonic distortion of around 0.1%. This confirms the neural network's ability to detect distortion and dynamically adapt its parameters to maintain high filtering performance, even under non-ideal grid conditions.

4 Conclusion

This research work presented an adaptive D-CSOGI-ANN synchronization system that dynamically adjusts to grid conditions in real time. Unlike the conventional fixed-gain D-CSOGI, the proposed structure employs a neural network to modify the filtering gain according to the harmonic content of the input signal. The simulation results demonstrated a faster dynamic response under clean conditions, as well as a notable improvement in harmonic rejection under distorted grids, reducing output THD to around 0.1% compared to 2.2% with a static design. These results confirm the effectiveness and real-time applicability of the proposed approach.

References

[1] B. Popadić, B. Dumnić, V. Katić, D. Šljivac, and D. Pelin, "Overview of grid connected converter synchronization techniques under different grid voltage conditions," *Proc. Int. Conf. Smart Syst. Technol. 2017, SST 2017*, vol. 2017-December, pp. 99–105, Dec. 2017, doi: 10.1109/SST.2017.8188677.

[2] R. Moutchou and A. Abbou, "Control of grid side converter in wind power based PMSG with PLL method," *Int. J. Power Electron. Drive Syst.*, vol. 12, no. 4, pp. 2191–2200, Dec. 2021, doi: 10.11591/IJPEDS.V12.I4.PP2191-2200.

[3] M. S. Nkambule, A. N. Hasan, A. Ali, and T. Shongwe, "A Novel Control Strategy in Grid-Integrated Photovoltaic System for Power Quality Enhancement," *Energies 2022, Vol. 15, Page 5645*, vol. 15, no. 15, p. 5645, Aug. 2022, doi: 10.3390/EN15155645.

[4] I. En-Naoui, A. Radouane, A. Mouhsen, E. Jarmouni, and E. Ennajih, "DSP implementation and discretization of phase locked loop methods in presence of grid imperfections," *Int. J. Power Electron. Drive Syst.*, vol. 15, no. 3, pp. 1490–1498, Sep. 2024, doi: 10.11591/IJPEDS.V15.I3.PP1490-1498.

[5] S. Natesan and J. Venkatesan, "A SRF-PLL Control Scheme for DVR to Achieve Grid Synchronization and PQ Issues Mitigation in PV Fed Grid Connected System," *Circuits Syst.*, vol. 07, no. 10, pp. 2996–3015, 2016, doi: 10.4236/CS.2016.710256.

[6] F. SEVİLMİŞ and H. KARACA, "Performance analysis of SRF-PLL and DDSRF-PLL algorithms for grid interactive inverters," *Int. Adv. Res. Eng. J.*, vol. 3, no. 2, pp. 116–122, Aug. 2019, doi: 10.35860/IAREJ.412250.

[7] A. Ghoshal Vinod John, A. Ghoshal, and V. John, "Performance evaluation of three phase SRF-PLL and MAF-SRF-PLL," *Turkish J. Electr. Eng. Comput. Sci.*, vol. 23, no. 6, pp. 1781–1804, Jan. 2015, doi: 10.3906/elk-1404-488.

[8] D. Wang, L. Yang, and L. Ni, "Performance and harmonic detection algorithm of phase locked Loop for parallel APF," *Energy Informatics*, vol. 7, no. 1, pp. 1–19, Dec. 2024, doi: 10.1186/S42162-024-00325-3/FIGURES/11.

[9] G. A. Herrejón-Pintor, E. Melgoza-Vázquez, and J. L. Monroy-Morales, "A Three-Phase Synchronization Algorithm Based on a Modified DSOGI with Adjustable Re-Filtering," *Energies 2023, Vol. 16, Page 6500*, vol. 16, no. 18, p. 6500, Sep. 2023, doi: 10.3390/EN16186500.

[10] A. A. Nazib, D. G. Holmes, and B. P. McGrath, "Decoupled DSOGI-PLL for Improved Three Phase Grid Synchronisation," *2018 Int. Power Electron. Conf. IPEC-Niigata - ECCE Asia 2018*, pp. 3670–3677, Oct. 2018, doi: 10.23919/IPEC.2018.8507364.

[11] A. Kulkarni and V. John, "Design of a fast response time single-phase PLL with DC offset rejection capability," *Conf. Proc. - IEEE Appl. Power Electron. Conf. Expo. - APEC*, vol. 2016-May, pp. 2200–2206, May 2016, doi: 10.1109/APEC.2016.7468172.

[12] S. Ke and Y. Li, "Analysis and modelling of a phase-locked loop based on a novel cascade structure of SOGI," *IET Power Electron.*, vol. 16, no. 15, pp. 2549–2559, Nov. 2023, doi: 10.1049/PEL2.12581.

[13] A. Kulkarni and V. John, "Design of a fast response time single-phase PLL with dc offset rejection capability," *Electr. Power Syst. Res.*, vol. 145, pp. 35–43, Apr. 2017, doi: 10.1016/J.EPSR.2016.12.023.

[14] E. Jarmouni, A. Mouhsen, M. Lamhamedi, H. Ouldzira, and I. En-Naoui, "Integration of an optimized neural network in a photovoltaic system to improve maximum power point tracking efficiency," *Indones. J. Electr. Eng. Comput. Sci.*, vol. 28, no. 3, pp. 1276–1285, Dec. 2022, doi: 10.11591/IJEECS.V28.I3.PP1276-1285.

[15] E. Hosseini, B. Saeedpour, M. Banaei, and R. Ebrahimy, "Optimized deep neural network architectures for energy consumption and PV production forecasting," *Energy Strateg. Rev.*, vol. 59, p. 101704, May 2025, doi: 10.1016/J.ESR.2025.101704.

[16] A.-N. Sharkawy, "The effect of increasing hidden layers on the performance of the deep neural network: modelling, investigation, and evaluation," *Res. Eng. Struct. Mater.*, Nov. 2024, doi: 10.17515/RESM2024.442ST0909TN.